УДК 537.86.029.65/.79

S. A. Kuznetsov [1, 2], **A. V. Arzhannikov** [1, 2], **A. V. Gelfand** [3], **V. V. Kubarev** [2], **M. Navarro-Cía** [4], **M. Beruete** [4], **F. Falcone** [4], **M. Sorolla** [4], **M. Thumm** [5, 1]

[1] Novosibirsk State University, Analytic and Technological Innovation Center "High technology and novel materials" Pirogova Str. 2, 630090 Novosibirsk, Russian Federation

[2] Budker Institute of Nuclear Physics SB RAS, Lavrentiev Ave. 11, 630090 Novosibirsk, Russian Federation
E-mail: S.A.Kuznetsov@inp.nsk.su

[3] Institute of Semiconductor Physics SB RAS, Novosibirsk Branch "TDIAM" Nikolaeva Str. 8, 630090 Novosibirsk, Russian Federation

[4] Millimeter and Terahertz Waves Laboratory, Universidad Pъblica de Navarra Campus Arrosadna, 31006 Pamplona, Spain

[5] Institute for Pulsed Power and Microwave Technology (IHM) and Institute of High Frequency Techniques and Electronics (IHE), Karlsruhe Institute of Technology (KIT), Kaiserstr. 12, D-76131 Karlsruhe, Germany

MICROSTRUCTURED QUASI-OPTICAL SELECTIVE COMPONENTS FOR SUBTERAHERTZ AND TERAHERTZ APPLICATIONS

The development results for passive quasi-optical selective components based on planar regularly patterned metallized microstructures of subwavelength topology are described. The components include different frequency filters, polarization beam-splitters, metastructures, thin resonant absorbers, which are elaborated both for stand-alone applications and for integration with various metrological systems used in subTHz and THz measurements. The methods for electromagnetic simulation, technological implementation, and components characterization are discussed.

Keywords: terahertz instrumentation, quasi-optical components, frequency-selective surfaces, filters, metamaterials, resonant absorbers, microstructures.

С. А. Кузнецов, А. В. Аржанников, А. В. Гельфанд, В. В. Кубарев, М. Наварро-Сиа, М. Берете, Ф. Фальконе, М. Соройа, М. Тумм

МИКРОСТРУКТУРНЫЕ КВАЗИОПТИЧЕСКИЕ СЕЛЕКТИВНЫЕ КОМПОНЕНТЫ ДЛЯ СУБТЕРАГЕРЦОВЫХ И ТЕРАГЕРЦОВЫХ ПРИЛОЖЕНИЙ

Описаны результаты разработки пассивных квазиоптических селективных компонентов на основе планарно-периодических металлизированных микроструктур субволновой топологии. Компоненты включают различные частотные фильтры, поляризационные делители, метаструктуры, ультратонкие резонансные поглотители, разработанные как для автономного использования, так и для работы в составе различных метрологических систем терагерцового и субтерагерцового диапазонов. Обсуждаются методы электродинамического моделирования, технологической реализации и инструментального тестирования разработанных компонентов.

Ключевые слова: терагерцовые измерения, квазиоптические компоненты, частотно-избирательные поверхности, фильтры, метаматериалы, резонансные поглотители, микроструктуры.

ISSN 1818-7994. Вестник НГУ. Серия: Физика. 2010. Том 5, выпуск 4
Vestnik Novosibirsk State University. Series: Physics. 2010. Volume 5, issue 4

Introduction

On the frequency scale of the electromagnetic spectrum the region of subterahertz and terahertz frequencies, extensively explored during the last decade, occupies a unique position due to its huge and still non-depleted potential for novel applications in physics, chemistry, biology, medicine, security etc [1]. In many cases a successful realization of (sub)THz-experiments demands adequate quasi-optical selective devices or components to control the properties of radiation beams. Such components implemented on basis of planar regularly patterned metallized microstructures (MMSs) of subwavelength topology, as a rule, serve as the best solution since their amplitude, phase and polarization response can be properly tailored via MMS topology, as well as the number of MMS layers used [1-4]. Compared to conventional optical elements [5], MMS-based components are advantageously thinner or much thinner than the operated wavelength λ, they are planar-profiled and their fabrication can be easily realized via a relatively cheap and well-proven photolithographic or other micromachining techniques of micrometer accuracy.

In this paper we briefly consider phenomenological properties of MMSs and methods for their development, as well as present selected results of MMS-components elaboration for different experimental tasks: harmonics filtering at the Novosibirsk THz-FEL, plasma diagnostics, realization of left-handed metamaterials, implementation of frequency selective bolometric detectors.

MMS phenomenology

Subwavelength MMSs have been studied and used in THz instrumentation since the end of 1960s, when R. Ulrich first investigated in detail the frequency responses of different metal mesh structures for the purpose of their application in quasi-optical submm-wave filters [2, 3]. The most important regime of MMS operation concerns the frequencies below the diffraction onset point, when only the fundamental reflection and transmission modes propagate under plane wave excitation: $\omega<\omega_{diff}$ (here $\omega=g/\lambda$, $\omega_{diff}=1/[1+\sin\theta]$; g is a lattice constant, θ is an incidence angle). In a *transmission line approach* (TLA), MMS is considered as a resonant LCR-circuit (or a set of circuits) shunting space, where MMS is placed and which serves as a transmission line for the propagating TEM waves. It is essential that the lumped circuit elements *L, C, R*, are specified by geometric parameters of the MMS micropattern and can be properly designed to provide a desired FSS's selectivity (Fig. 1).

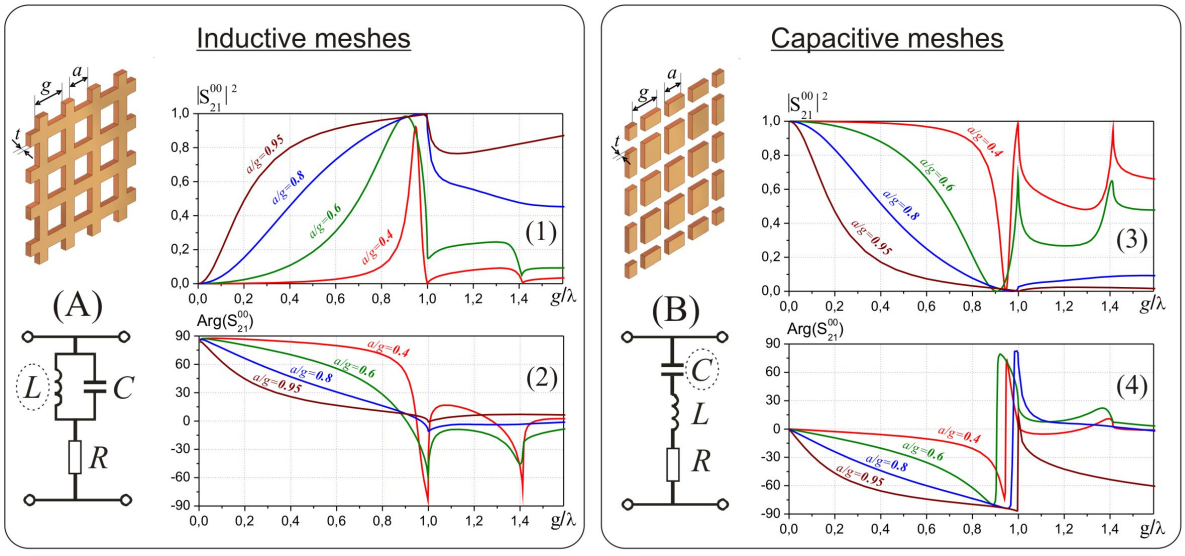

Fig. 1. Illustration of the lumped circuit representation for single inductive (A) and capacitive (B) meshes. Graphs (1), (3) and (2), (4) reproduce simulated in Ansoft HFSS™ spectral transmission $|\mathbf{S}_{21}|^2$ and transmission phase $\mathrm{Arg}(\mathbf{S}_{21})$ of the fundamental Floquet mode for substrate-free thin copper meshes with square cell topology at different values of the filling factor a/g (metallization thickness: $t/g=1\cdot10^{-3}$; normal excitation)

MMSs are usually sort into *capacitive* (C) and *inductive* (I) topologies, which differ either MMS unit cells are electrically isolated or not on a wavelength (or smaller) scale respectively. According to the Babinet's principle, C-MMS and I-MMS of complementary geometries manifest complementary frequency response (Fig. 1). At low frequencies ($\omega<<1$) C-MMS is radiation-transparent, while I-MMS is opaque that in a TLA-representation corresponds to capacitive or inductive MMS reactance respectively. As ω grows, I-MMS's transmissivity $|\mathbf{S}_{21}|^2$ (or C-MMS's reflectivity $|\mathbf{S}_{11}|^2$) steadily increases up to the point $\omega_{res}\cong(LC)^{-1/2}$ of resonant transmission (or reflection for C-MMS), which for a simple MMS with regular-polygon-shaped cells lies slightly below the diffraction point ω_{diff}. This resonance is associated with a *"plasmon-polariton"* mechanism [6] originated from MMS periodicity and explained by the effective excitation of evanescent surface waves [1] in the vicinity of ω_{diff} that leads to resonant amplification of the near-field on the MMS unit cells, interfering constructively (or destructively) in the far-field. The plasmonic resonance is very sensitive to the oblique incidence (Fig. 2) that limits application of simple MMSs in band-pass or band-stop spectral filtering, though their employment as high-pass or low-pass filters is very effective [2, 3].

To improve the angular stability of MMS characteristics, the LC-resonance should be shifted to the lower frequencies by increasing MSS's intra- or inter-cell capacitance or (and) inductance via modifying the MMS micropattern. Such MMS with more sophisticated topology, which specifies a type, form and number of desired low-frequency LC-resonances, are known as *selfresonant* MMSs or *frequency selective surfaces* (FSSs) [4]. Compared to the aforementioned plasmon-polariton resonance, the near-field amplification in a FSS resonance is essentially realized, as a rule, not via surface wave pumping, but through exciting a standing wave on the FSS unit cell. E.g. for a substrate-free FSS with frequently employed narrow line- or cross-shaped dipole elements of the length a (Fig. 3), the fundamental resonance

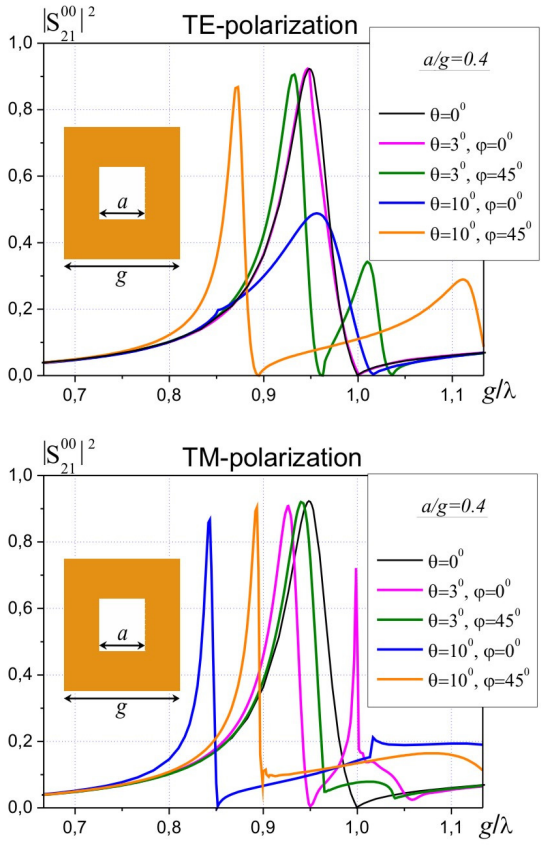

Fig. 2. Plasmonic resonance sensitivity to changing the angles of incidence θ, φ: an example of the inductive mesh with square holes (a/g=0.4)

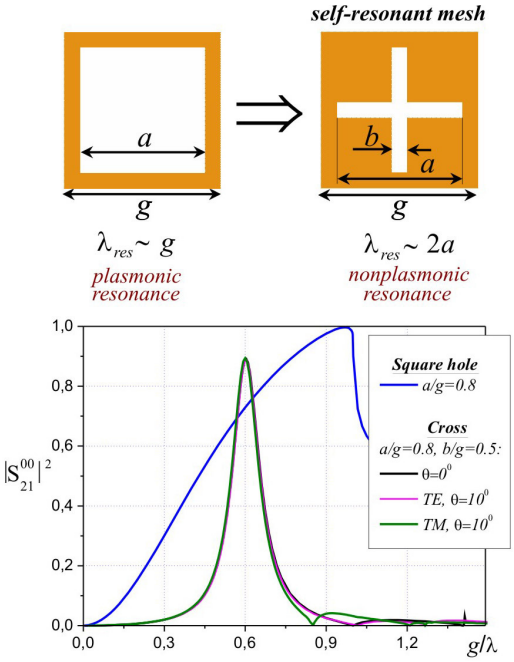

Fig. 3. Improving angular stability of the I-MMS resonance through topology modification: *square hole* → *cross*. Increased capacitance for the cross-shaped holes yields the red-shift of the resonant frequency $\omega_{res}\cong(LC)^{-1/2}$ and the decrease of the resonance bandwidth

[1] Predominantly, ±1 diffraction harmonics, which are bounded to the surface due to the ban on their free-space propagation at $\omega<\omega_{diff}$.

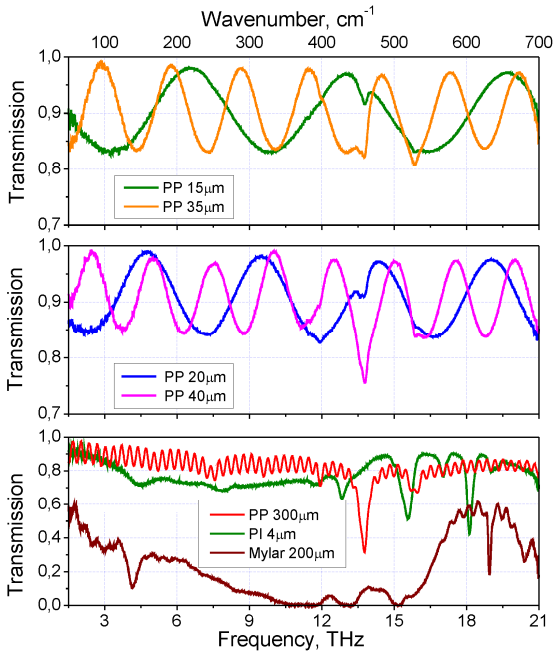

Fig. 4. Terahertz properties of some commercial polymeric films (Bruker™ IFS 66 v/s characterization). The distinctive Fabry-Perot modulation of the transmission at ~97-99% peak values for PP films 15-40 μm thick demonstrates their low dispersion and low losses ($\tan\delta \sim 1 \div 2 \cdot 10^{-3}$)

corresponds to a half-wave excitation mode: $\lambda_{res}/2 \sim a$ (this enables shifting ω_{res} almost twice below ω_{diff}) [2].

Last years MMSs gained a new impetus due to development of the *electromagnetic metamaterials* concept [7, 8], in which FSSs with very low frequency (quasi-static) resonances are considered. Compared to MMS-filters typically based on FSSs with g~0.3-0.8 λ_{res}, the stacked meta-FSSs are exploited in the regime $g \ll \lambda_{res}$ that allows considering individual FSS-cells as artificial "atoms" and describe such complex media in terms of the effective homogenized ("bulk-like") permeability μ_{eff} and/or permittivity ε_{eff}, which can be properly engineered through the meta-cell topology. The most attractive regime concerns simultaneously negative values of μ_{eff} and ε_{eff} that is unachievable in natural media and yields left-handedness for the wave triplet (**k**, **E**, **H**) of the propagating EM-wave. In such *left-handed media* the effective refractive index $n_{eff} = -(\mu_{eff} \cdot \varepsilon_{eff})^{1/2}$ is negative that causes antiparallelism of the group and phase velocities (*backward wave propagation*) and opens up possibility for *electromagnetic cloaking* and *superlensing*, as well as for some other spectacular electromagnetic phenomena [7, 8].

THz-MMS development: methods and techniques

In our research-and-development activities, elaboration of MMS-based components for operation at subTHz and THz frequencies is fulfilled in a cycle of the consecutive stages: *EM-modelling* → *Fabrication* → *Characterization.* The methods and techniques employed at each stage are described below.

Electromagnetic modelling

The commercial electromagnetic simulators *Ansoft HFSS*™ (Finite Elements Method) and *CST Studio Suite*™ (Finite Integration Technique) [9] are used for a full-wave 3D EM analysis and design optimization of MMS-components with the required selective properties [3]. For simulating a regularly patterned MMS as an infinite periodic cell array, the Floquet port excitation regime and periodic boundary conditions are applied to an MMS's unit cell. It allows an accurate calculation of the S-parameters of the periodic structure both below and above the diffraction onset point ω_{diff}.

Fabrication

As for (sub)THz MMSs the typical topological dimensions of its micro-pattern lie within the scale ~3-300 μm, a standard *contact photolithography technique* (CPhLT) can be effec-

[2] The resonance bandwidth $\Delta\omega/\omega_{res}$ substantially depends on the width b of dipole elements: $\Delta\omega/\omega_{res} \to 0$ if $b \to 0$. The decrease of b yields the increase of MMS-cell capacitance C_{ind} (for I-MMS) or inductance L_{cap} (for C-MMS) that results in diminishing $\Delta\omega/\omega_{res}$ according to the TLA's relationships: $\Delta\omega/\omega_{res} \approx 2 \cdot (L_{ind}/C_{ind})^{1/2}/\eta_0$ – for I-MMS, and $\Delta\omega/\omega_{res} \approx \frac{1}{2}\,\eta_0 \cdot (C_{cap}/L_{cap})^{1/2}$ – for C-MMS (η_0 is a free-space impedance).

[3] In some cases the aforementioned transmission line approach is also employed to accelerate optimization of the multi-layer MMSs, though TLA itself does not give the spectral behavior of the lumped circuit parameters *L, C, R.* The latter can be derived from the full-wave electromagnetic analysis.

tively used for MMS fabrication. In this work we adapted CPhLT for manufacturing MMSs on the surface of low-absorbing polymeric films metallized by 0.4 μm thick aluminum via a thermal vacuum deposition method. Two polymers were chosen for THz applications due to their satisfactory technological and optical characteristics: polyimide (PI) and polypropylene (PP). Compared to PI, PP exhibits very low dispersion and dielectric losses within a very wide frequency range (Fig. 4) and suits for fabricating multilayered MMSs by a hot pressing technique, whereas PI has higher mechanical fastness and thermostability and is ideal for high-quality thin film growing from a liquid phase by spin coating and thermal annealing processes inappropriate for PP (see [10, 11] for details). The minimal tested topological size of the output MMS samples is estimated as 2.5-3 μm at clear aperture diameter up to ∅80 mm. Along with CPhLT, we also focus on mastering the technologies based on *deep X-ray lithography* and *electroforming techniques*, which are intended for the fabrication of thick substrate-free self-bearing inductive MMSs of medium and high aspect ratios [12]. Such MMSs are promising for application under high-power load conditions (e.g. in FEL experiments) when polymeric film backed THz-MMSs become unsuitable due to the danger of their thermal destruction. Additionally, the substrate-free MMSs exhibit potentially smaller intrinsic losses due to absence of dielectric layers.

Characterizatio

To measure the frequency selective properties of the fabricated MMSs, three different quasi-optical frequency-domain spectrometers overlapping the total frequency range *0.04-21 THz* are used. Each spectrometer briefly described below differs in the instrumentation scheme and is intended for specialized measurements within its peculiar frequency subrange.

1) AB Millimeter™ Vector Network Analyzer MVNA-8-350-4 [13]. Equipped with a quasi-optical bench for free-space measurements, this dual channel MVNA enables to obtain the complex transmission and reflection coefficients (4S-parameters) of the samples under test at the frequencies *f=41-670 GHz*. The MVNA is built on all solid-state electronics basis, in which subTHz waves are generated by the frequency multiplication of the coherent signal from a tunable microwave source (8.0-18.8 GHz) and are detected by harmonic mixing. The multiplication-detection functions are performed in the Shottky-diode-based millimeter heads, while the detected signals are processed by a heterodyne vector receiver with an internal reference channel that eliminates the need of a dual-beam interferometer configuration for the phase gauging. A linearly polarized Gaussian beam is generated by a horn antenna, focused by ellipsoidal mirrors upon the investigated sample and guided afterwards by two identical ellipsoidal mirrors towards the receiver horn antenna. The typical values of spectral, amplitude and phase resolution of MVNA are better than 25 MHz, 0.01 dB and 0.01° respectively, while its dynamic range is ~110 dB for f <110 GHz, decreasing to ~60 dB at the higher-frequency edge.

2) Quasi-Optical BWO-Spectrometer [14]. This hybrid type instrument combines the elements of microwave technique and FIR spectroscopy. A set of monochromatic electronically tunable Backward Wave Oscillators (BWOs) is used to overlap the frequency range *0.1-1.5 THz* in this spectrometer. The Golay-cell detector combined with a lock-in amplifier is employed for registering a 23 Hz-modulated THz beam collimated by dielectric lenses. The optical scheme of the dual path Mach-Zehnder (Michelson) interferometer with a controlled movable mirror is used for measuring a transmission (reflection) phase. The relative frequency resolution and dynamic range of the spectrometer are 10^{-5} and 40-60 dB correspondingly at a few per cent accuracy for amplitude and phase measurements.

3) Bruker™ Vacuum Fourier Spectrometer IFS 66v/s [15]. This instrument uses a well-proven spectroscopic technique in which the transmission or reflection spectra are obtained via a Fourier transform procedure applied to the interferometric signal from the detector in a dual-beam Michelson interferometer. The detected signal is recorded as a function of the movable mirror position in the variable arm of the interferometer. Compared to the aforementioned spectrometers, the broadband thermal radiation sources are employed in this instrument that provides extremely wide total frequency coverage: 10-4000 cm^{-1} at spectral

resolution 0.12 cm^{-1}. Typically, for THz measurements we use the band 35-700 cm^{-1} (*1-21 THz*) by exploiting an easy-to-use room-temperature pyroelectric detector, which provides up to 30 dB of the dynamic range at a few per cent amplitude accuracy. For the higher sensitivity measurements the helium- and nitrogen-cooled detectors are available. It is also important that this spectrometer is capable of measuring under vacuum pumping conditions to avoid parasitic absorption of THz radiation in ambient atmosphere (mainly, due to rotational transitions in H_2O molecules), which severely deteriorate measurements at frequencies above 1.5 THz.

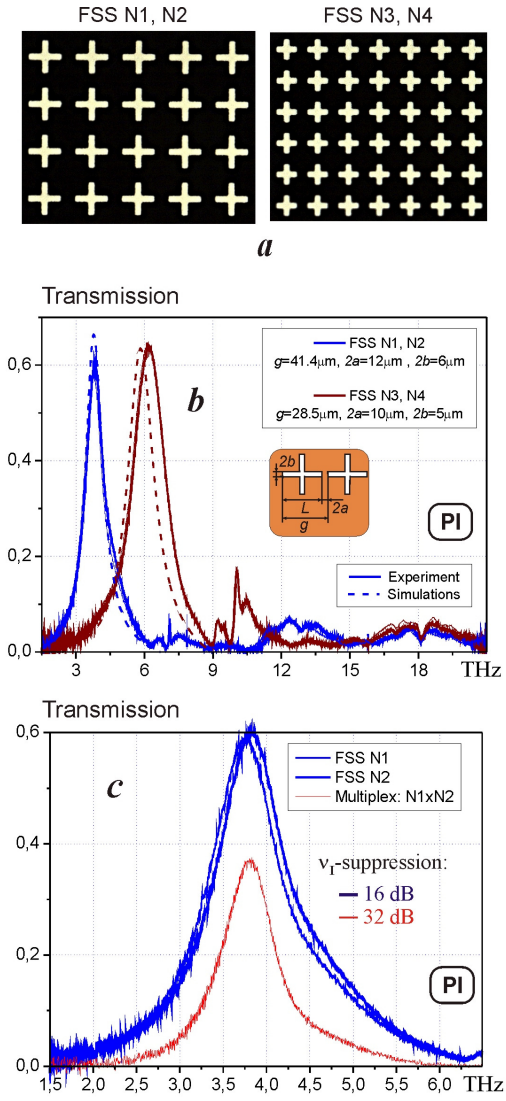

Fig. 5. Micropattern photographs for the fabricated 3.5μm-PI-backed FSSs with topology of "inductive crosses" (a) and their band-pass properties (b, c)

Examples of the developed MMS-components

Single-layer frequency filter

By using CPhLT, we have successfully fabricated and tested a set of single-layered FSS filters intended for filtering radiation harmonics from the first line of Novosibirsk terahertz free electron laser (NovoFEL), which generates the fundamental radiation mode within a spectral range 1.3–2.5 THz [16]. Fig. 5, 6 illustrate the topological pattern and spectral response of the developed band-pass and band-stop filters utilizing the topologies of "inductive crosses" and "capacitive rings" respectively. The inductive FSSs were implemented on basis of the PI films 3.5μm thick and were optimized for the band-pass selection of the 2nd and 3rd NovoFEL harmonics with frequencies $\nu_{II} \cong 4$ THz and $\nu_{III} \cong 6$ THz against a background of the fundamental generation mode $\nu_I \cong 2$ THz, whereas the capacitive 20μ-PP-film-backed FSSs were designed for the resonant rejection of ν_I at 2.3 THz. At the initial stage of the design optimization the resonant wavelengths of "crosses" (+) and "rings" (o) were estimated from the approximate relations: $\lambda_{res\,(+)} \approx 2L \cdot n_{eff}$, $\lambda_{res\,(o)} \approx \pi d \cdot n_{eff}$, where $n_{eff} = [(\varepsilon+1)/2]^{1/2}$ is an effective refractive index for the air-dielectric interface (ε – substrate permittivity: $\varepsilon_{PP} \cong 2.25$, $\varepsilon_{PI} \cong 3.24$).

From the Fig. 5b, c it can bee seen that despite the small thickness of PI, its high dielectric losses ($\tan\delta \sim 0.04$) result in a noticeable degradation of the FSS transmittance. This drawback, which limits application of PI in multilayer structures, can be overcome by employing PP substrates. Alternatively, in case of substrate-free inductive MMSs the losses can be further minimized. The examples of such self-bearing nickel MMSs with round hexagonally packed openings a few ten microns thick are shown in Fig. 7. The MMSs exhibit quasi-band-pass characteristics and destined for filtering applications in NovoFEL experiments.

Bi-layer interference frequency filters

To improve the band-selective properties of FSS-filters, the number of FSS layers should be greater than one. It's important to note that compared to the multiplex FSS-filters, in which

the cross-interference between the adjacent FSS layers is suppressed due to their proper angle misalignment, the interference configurations with quarter-wavelength interlayer separation allow to obtain the steeper edges of the selection band (see e.g. Fig. 9).

Fig.8 illustrates our first results on development of the bi-layer band-pass interference filters based on PP-film-backed FSSs designed for application in a 4-channel radiometric diagnostics of 240-420 GHz emission from turbulent plasma at the GOL-3 nuclear fusion facility [17, 18]. FSSs with anisotropic topology ("inductive slots") were used to provide ~40 GHz frequency shift of the transmission bands for orthogonally polarized radiation components. It let us to employ only two FSS-structures for realizing 4 spectral channels that reduced the total fabrication costs. A hot lamination technique was employed to fuse 40μm-PP-films for creating the designed multistack configurations. We also found that despite high quality of the used PP substrates the hot lamination procedure had induced microcracks in 0.4μm-Al-metallization, as well as caused uncontrollable deviation of the topological parameters, that explains degradation of the peak transmittance down to 44-52%. Currently, we are focused both on mastering the thermal fusion process for producing PP-based FSS-filters and on implementation of substrate-free copper-based MMSs manufactured via electroforming (Fig. 9).

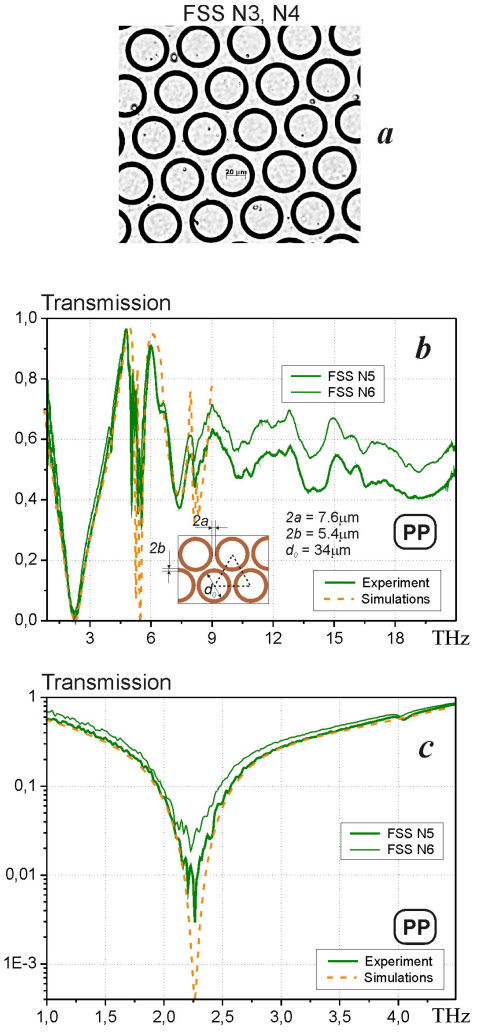

Fig. 6. Micropattern photograph for the fabricated 20μm-PP-backed FSSs with topology of "capacitive rings" (a) and their band-stop properties (b, c)

Polarization beam-splitter

The fine-structure free-standing 1-D metallic grids (with a grid pitch $g/\lambda<<1$) are effectively employed for polarization demultiplexing of THz beams, as well as for radiation polarization analysis and intensity control [14]. For the purpose of submm-wave plasma diagnostics applications [17, 18], in our work a series of beam-splitters utilizing the grids with a pitch g=8 μm and ~50% metal filling were photolithographically fabricated on the surface of 20μm-PP-film substrates with clear aperture diameter ∅80 mm. At the frequencies below 500 GHz the beam-splitters demonstrated the attenuation factor >32 dB for the E-polarized radiation component and total transparency for the case of H-polarization (Fig.10 a). The structures performance remains high up to the frequencies ~ several THz (Fig.10 b). We also found that similar beam-splitters based on

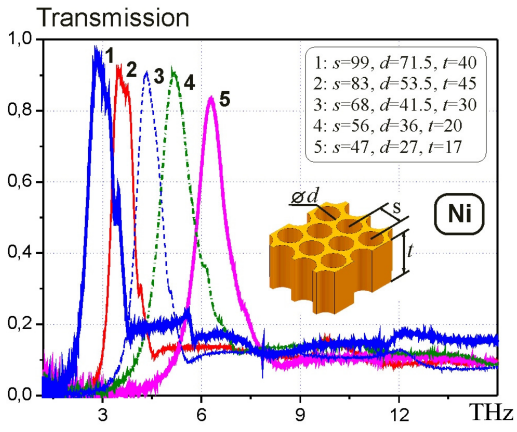

Fig. 7. THz-response of substrate-free electroformed nickel meshes. The units in the inset indicate microns

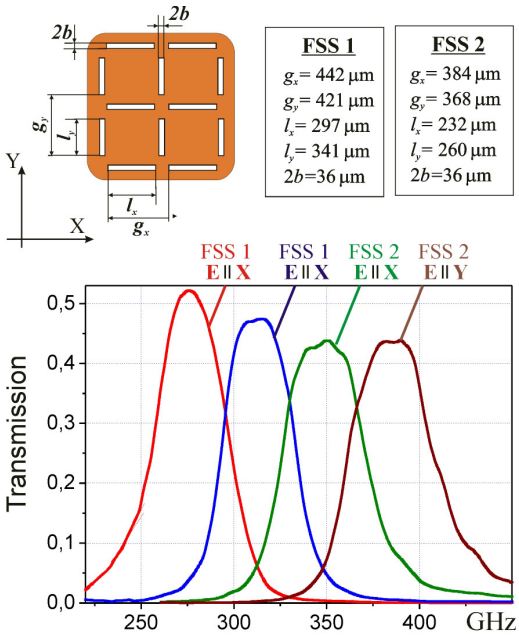

Fig. 8. Topological parameters and subTHz-response for bi-layer FSS-filters of the following configuration: *8x40μmPP+FSS+4x40μmPP+FSS+8x40μmPP*

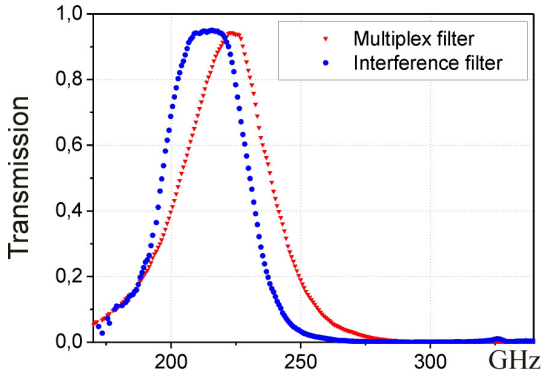

Fig. 9. Comparison of the band-pass selectivity for the bi-layer multiplex and interference FSS-filters

4μm-PI-film substrates exhibited the better efficiency at the frequencies < 5 THz. This fact is explained by intrinsically higher structural quality of the PI material compared to PP that diminishes technological errors during the fine-structure MMS fabrication.

Metamaterial structures

As it was mentioned above, artificial media with desired magnetic/electric response can be

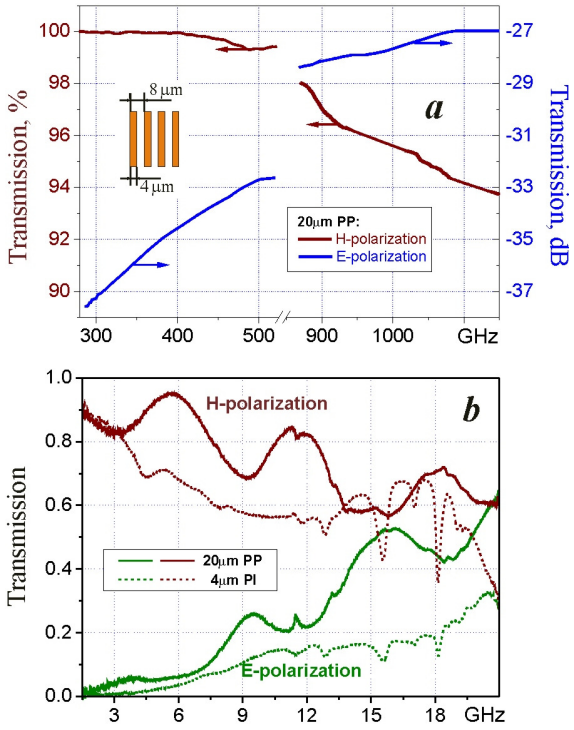

Fig. 10. Results of BWO- (a) FT-characterization (b) of the polarization beam-splitters

effectively realized on basis of FSSs with proper quasi-static magnetic/electric resonances. E.g. *split ring resonators* (SRR) are a well-known type of subwavelength particles used to obtain media with negative μ_{eff}. By employing SRR, the conventional approach to achieve the negative index of refraction is to combine SRR with a wire medium (the latter provides negative ε_{eff}) [7]. The alternative method is based on using stacked *complimentary split ring resonators* (CSRR), the SRR's counterpart, which exhibit left-handed propagation due the excitation of *electroinductive waves* (EIW) [19].

In our work we experimentally investigated the SRR and CSRR metasurfaces in single- and bi-layer configurations, whose funda-mental resonance was designed to be set in proximity of 66-68 GHz (Fig. 11, 12) [11, 20]. The good performance of the developed structures let us be confident in high prospects of PP substrates for subTHz metamaterials implementation. By the example of CSRR, we also demonstrated a feasibility of strong beam deceleration (more than two orders of magnitude), when CSRR layers are directly coupled via EIW [11] (Fig. 12).

Another attractive class of MMSs capable of supporting backward EIW is based on stacked subwavelength *hole arrays* (HAs) operating in the regime of *extraordinary transmission* (ET), i.e. when the hole's cut-off frequency lies higher than the plasmon-polariton resonance [21]. In such structures (Fig. 13), positioning between photonic crystals and "true" 3D metamaterials, the HAs act as electrically coupled cut-off artificial waveguides, whose dispersion parameter $\omega/\beta_z \cdot (\partial\omega/\partial\beta_z)$ can be tuned from positive to *negative* values through the proper control of the hole diameter, in-plane periodicities and inter-layer gap (hereinabove ω is the angular frequency and β_z is the propagation constant along the HA stacking direction). In Fig. 13e, f it is shown an example of a negative refraction prism carved from 15 ET-HA layers optimized to have the effective refractive index n_{eff}=-1 at 53.3 GHz (Fig. 13d). At difference with conventional dielectric prisms, the present design covers negative angles of refraction at the ET operation. Moreover, refraction is positive for the second band, so with a single structure all the output angles can be covered. Further adaptation of this approach to terahertz frequencies is in progress [22].

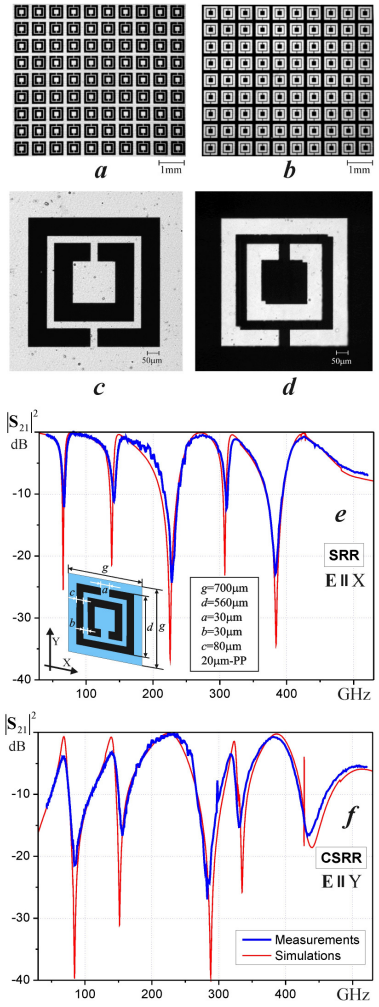

Fig. 11. Micropattern photographs for SRR (a, c) and CSRR (b, d) metasurfaces (*black corresponds to metal*). Co-polar transmission for single-layer 20μm-PP-backed SRR (e) and CSRR (f).

Ultrathin resonant absorbers

The topic of electrically thin artificial ground planes with high surface impedance, also known as *high-impedance surfaces* (HISs) or *artificial magnetic conductors*, has been intensively elaborated by antenna engineering and metamaterial communities [8]. Along with antenna applications, wherein energy dissipation is typically minimized, HISs also offer an effective solution for realization of the alternative operation regime: the high or *perfect resonant absorption* when the dielectric or ohmic losses are properly incorporated into the frequency-selective surface of the HIS [23]. The latter feature is estimated to be extremely attractive for its utilization in high-efficient and ultra-compact frequency-selective bolometric detectors operating in the THz band. It is essential that the large wavelength-to-thickness ratio λ/d of the HIS-based absorber ($\lambda/d >> 1$) allows minimizing its heat capacity and therefore increasing the operating speed and sensitivity of the bolometric detector.

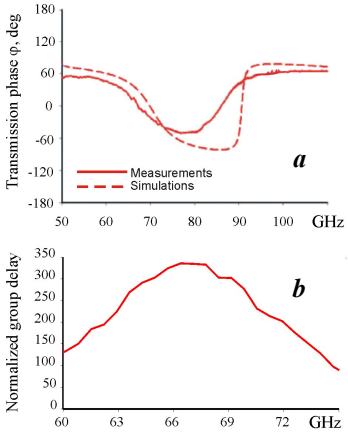

Fig. 12. Co-polar transmission phase (a) and derived group delay - $d\varphi(\omega)/d\omega$ (b) for the bi-layer CSRR stack normalized to the EM-wave delay in free space

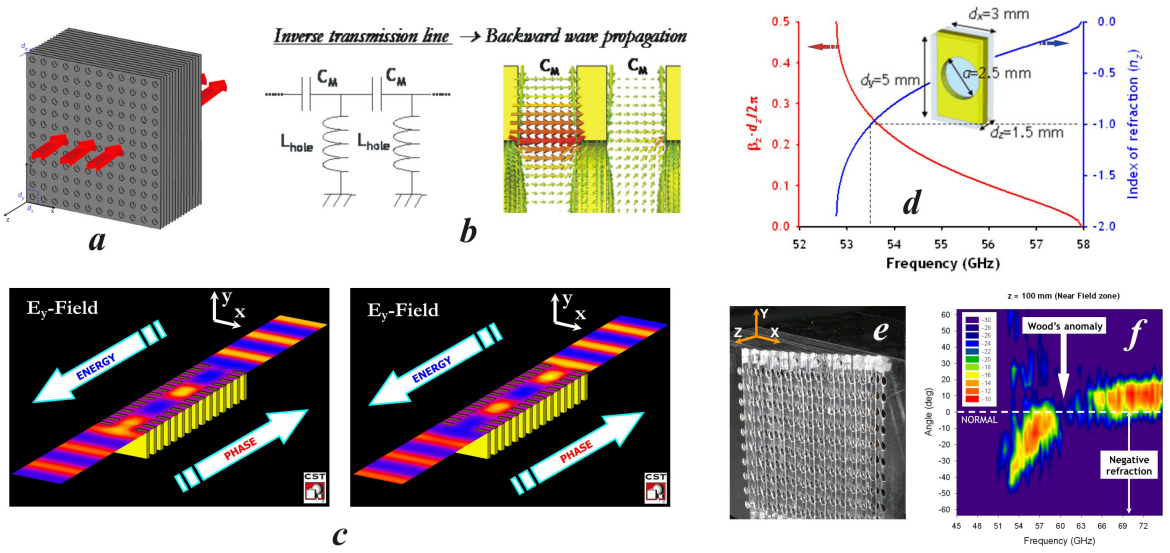

Fig. 13. Schematic of stacked ET-HA MMS (a). The strong capacitive coupling between adjacent inductive MMS layers via a normal component of the electric field (b) corresponds to formation of the inversed transmission line necessary for left-handed propagation (c). Example of the simulated dispersion diagram (d), and photograph of the metamaterial prism composed of 15 ET-HA layers (e) exhibiting negative refraction under ET operation (f)

In our work a series of different ultrathin HIS absorbers implemented in a "FSS + grounded PP slab" configuration were proposed and examined in the range of millimeter-submillimeter waves [24]. Fig. 14 illustrates the structure and performance for two types of narrow-band absorbers employing FSS with the topologies of split ring resonators (a, b) and a novel FSS comprised by densely packed convoluted tripole elements of a capacitive kind (DPFSS, c, d). It is noteworthy that despite the use of the low-loss dielectric substrates and high conductivity Al metallization it is feasible to realize close to unity absorptivity within a narrow resonant band. For the presented structures the relative spectral width of the fundamental absorption band is evaluated as 3% (SRR) and 8% (DPFSS) at the λ/d-ratio 47 and 64 respectively.

Currently, we elaborate the high-performance absorbers for novel bolometric matrix detectors [25] optimized for operation at the frequencies 0.3-1.5 THz.

Conclusion

Microstructured quasi-optical selective components are the essential part of instrumentation in modern terahertz research. In our work we successfully combine and exploit the basic methods and techniques to simulate, fabricate and characterize different MMS-components destined both for stand-alone applications and for integration with various metrological systems used in subTHz and THz measurements. In our rapidly developing activity we constantly make the efforts to improve the performance of our products, as well as to deepen and expand the area for their application.

This work is partially supported by the grant RNP 2.1.1/3983 of the Russian Ministry of Education and Science, the grant 11.G34.31.0033 of the Russian Federation Government, and the contract 16.740.11.0377 via the Federal Target Program.

References

1. *Yun-Shik L.* Principles of Terahertz Science and Technology // Springer. 2009.

2. *Ulrich R.* Far-Infrared Properties of Metallic Mesh and Its Complimentary Structure // Infrared Physics. 1967. Vol. 7. P. 37–55.

3. *Ade P.A.R. et al.* A Review of Metal Mesh Filters // Proc. SPIE. 2006. Vol. 6275. P. 62750U-1–62750U-15.

4. *Munk B.* Frequency Selective Surfaces: Theory and Design // NY: Wiley. 2000.

5. *Saleh B.E.A., Teich M.C.* Fundamentals of photonics // NY: Wiley. 1991.

6. *Pendry J. B. et al.* Mimicking Surface Plasmons with Structured Surfaces // Science. 2004. Vol. 305. P. 847–848.

7. *Eleftheriades G. V., Balmain K. G.* Negative Refraction Metamaterials: Fundamental Principles and Applications // Wiley and IEEE Press. 2005.

8. *Engheta N., Ziolkowski R.W.* Electromagnetic Metamaterials: Physics and Engineering Explorations // Wiley and IEEE Press. 2006.

9. On-line information: www.ansoft.com and www.cst.com.

10. *Kuznetsov S. A. et al.* Development and Characterization of Quasi-Optical Mesh Filters and Metastructures for Subterahertz and Terahertz Applications // Key Eng. Materials. 2010. Vol. 437. P. 276–280.

11. *Navarro-Cía M. et al.* A Route for Bulk Millimeter Wave and Terahertz Metamaterial Design // IEEE Journal of Quantum Electronics. 2010 (in press).

12. *S. A. Kuznetsov et al.* Development of copper meshes for frequency and spatial selection of the terahertz radiation of the Novosibirsk free electron laser // J. Surf. Investigation. X-ray, Synchrotron and Neutron Techniques. 2009. Vol. 3. No. 5. P. 691–701.

13. www.abmillimetre.com

14. *Kozlov G. V., Volkov V. V.* Coherent Source Submillimeter Wave Spectroscopy // Millimeter and Submillimeter Wave Spectroscopy of Solids (Topics in Applied Physics. Vol. 74) / Ed. by G. Gruener. Berlin; Heidelberg: Springer-Verlag. 1998. P. 51–109.

15. www.bruker.com

16. *Kulipanov G. N. et al.* Research highlights from the Novosibirsk 400 W average power THz FEL // Terahertz Science and Technology. 2008. Vol. 1. No. 2. P. 107–125.

17. *Kuznetsov S. A. et al.* Quasi-Optical Spectral System for Submm-Wave Radiometry of Turbulent Plasma // Proc. of 39th European Microwave Conf. 2009. P. 173–176.

18. *Kuznetsov S. A. et al.* Multichannel radiometric system for registering submillimeter-wave radiation at beam-plasma interaction // NSU Bulletin. Series: Physics. 2010. Vol. 5. Iss. 3. P. 5–19.

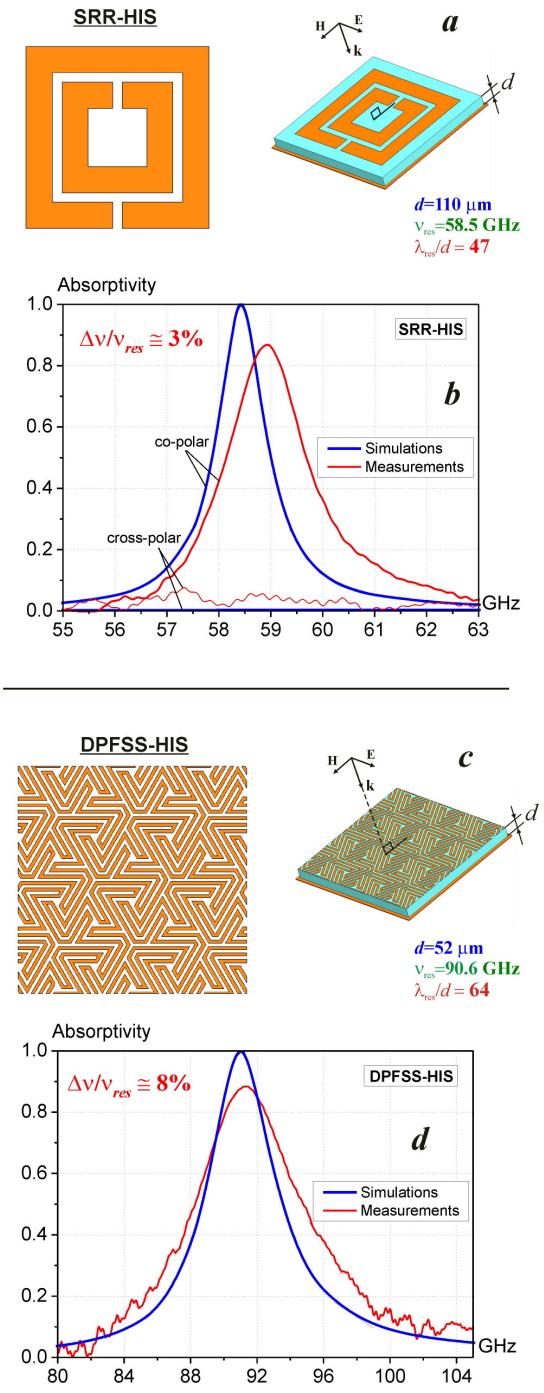

Fig. 14. Examples of mm-wave ultrathin HIS absorbers based on polarization-sensitive SRR (a, b) and polarization-insensitive DPFSS (c, d). Metallization corresponds to orange. The structures are shown in a true relative scale. For DPFSS the width of all topological lines is 10 μm at the triangular lattice constant g=230 μm, while the SRR array has a square cell packaging with g=700 μm

19. *Beruete M. et al.* Electroinductive waves role in left-handed stacked complementary split rings resonators // Optics Express. 2009. Vol. 17. Iss. 3. P. 1274–1281.

20. *Aznabet M. et al.* Polypropylene-Substrate-Based SRR- and CSRR-Metasurfaces for Submillimeter Waves // Optics Express. 2008. Vol. 16. Iss. 22. P. 18312–18319.

21. *Beruete M. et al.* Extraordinary Transmission and Left-Handed Propagation in miniaturized stacks of doubly periodic subwavelength hole arrays // Optics Express. 2007. Vol. 15. Iss. 3. P. 1107–1114.

22. *Kuznetsov S. A. et al.* Regular and Anomalous Extraordinary Optical Transmission at the THz-gap // Optics Express. 2009. Vol. 17. Iss. 14. P. 11730–11738.

23. *McVay J. et al.* Thin Absorbers Using Space-Filling-Curve Artificial Magnetic Conductors // Microw. Opt. Tech. Lett. 2009. Vol. 51. Iss. 3. P. 785–790.

24. *Kuznetsov S. A. et al.* Ultra-thin subterahertz absorbers based on high-impedance metasurfaces // Proc. of 4th Int. Congress on Advanced Electromagnetic Materials in Microwaves and Optics ("Metamaterials-2010"). 2010. P. 119–121.

25. *Gelfand A. V. et al.* Uncooled matrix IR detector based on optoacoustic cells and optoelectronic reading system // Opt. Memory & Neural Networks. 2009. Vol. 18. No. 1. P. 25–28.

28.09.2010